

Long-living Bloch oscillations of matter waves in optical lattices

M. Salerno¹, V. V. Konotop^{2,3}, and Yu. V. Bludov³

¹*Dipartimento di Fisica E. R. Caianiello, and Consorzio Nazionale Interuniversitario per le Scienze Fisiche della Materia (CNISM), Università di Salerno, I-84081, Baronissi (SA), Italy*

²*Departamento de Física, Universidade de Lisboa,*

Campo Grande, Edifício C8, Piso 6, Lisboa 1749-016, Portugal

³*Centro de Física Teórica e Computacional, Universidade de Lisboa,*

Complexo Interdisciplinar, Avenida Professor Gama Pinto 2, Lisboa 1649-003, Portugal

It is shown that by properly designing the spatial dependence of the nonlinearity it is possible to induce long-living Bloch oscillations of a localized wavepacket in a periodic potential. The results are supported both by analytical and numerical investigations and are interpreted in terms of matter wave dynamics displaying dozens of oscillation periods without any visible distortion of the wave packet.

PACS numbers: 03.75Kk, 03.75Lm, 67.85.Hj

The phenomenon of Bloch oscillations (BO), predicted by Bloch in 1928 in his celebrated paper on the dynamics of a band electron in a steady electrical field [1], represents a problem of non exhausted interest. Besides solid state physics, where the phenomenon has been observed only in recent times after the development of the superlattice technology [2], it is now possible to observe BO also in other fields such as nonlinear optics, using light beams in arrays of waveguides [3] or in photorefractive crystals [4], and atomic physics, using Bose-Einstein condensates (BEC) loaded in optical lattices (OLs) [5, 6, 7]. Apart its fundamental significance, the interest in BO arises mainly from perspectives of their practical applications. In this context we mention the use of BO for metrological tasks, including relatively precise definition of h/m [8] and measurement of forces at the micrometer scale like the Casimir-Polder force [9] and the gravity [10]. Recently, BO were also suggested as a tool for controlling light in coupled-resonator optical waveguides [11]. In these physical contexts BO have been observed mainly in the linear (as first proposed by Bloch) or quasi linear regimes (where the nonlinearity introduces quantitative but not yet qualitative changes). The present experimental settings (both in nonlinear optics and in BECs), however, allow for attaining essentially nonlinear regimes quite easily, this actually being a desirable condition for applications involving localized states.

The fact that BO can exist in presence of interactions (nonlinearity) was first recognized in the context of nonlinear discrete systems [12]. For periodic continuous models of the nonlinear Schrödinger (NLS) type, such as ones describing matter waves in OLs, the existence of BO becomes more problematic because of nonlinearity induced instabilities in the underlying linear system. These instabilities can be simply understood by observing that in a usual OL at the edges of an allowed band the effective mass has always opposite signs. This implies that if a Bloch state is modulationally stable (in

presence of a constant nonlinearity) at one edge of the band, it must be necessarily unstable at the other band edge [13]. Nonlinearity induced instabilities have been extensively investigated both theoretically [13, 14] and experimentally [15]) and have been identified as primary cause for the short life-times of BO of matter waves (the oscillation survives only a few cycles) observed both in numerical [16] and in real experiments [15].

In this Letter we show that by properly controlling the instabilities of the system it is possible to achieve long-living BO of matter waves in OLs. In our approach BO are implemented using solitonic propagation (the situation similar to one explored in truly discrete systems [12]). To this end we use spatial periodic modulations of the scattering length via optically induced Feshbach resonances, in order to change the stability properties of the Bloch states at the edges of the band. These modulations correspond to a nonlinear lattice whose amplitude, considered as a free parameter, can be used to eliminate instabilities from the band (similar stabilizing properties of nonlinear lattice were used to achieve delocalizing transitions in one dimensional (1D) case [17]). We show that the regions of parameter space for which Bloch states become unstable (almost) in the whole band coincide with those for which long-lived BO of matter waves become possible, this showing the validity of our approach.

We start by considering the following 1D Gross-Pitaevskii equation

$$i\psi_t = -\psi_{xx} + \gamma x\psi + \mathcal{U}(x)\psi + \mathcal{G}(x)|\psi|^2\psi, \quad (1)$$

describing an array of BECs in linear and nonlinear π -periodic optical lattices of the form $\mathcal{U}(x) = \mathcal{U}(x + \pi)$, $\mathcal{G}(x) = \mathcal{G}(x + \pi)$, respectively, with the external linear force γ arising from an uniform acceleration of the lattices (a similar approach is valid also for the multidimensional case). The consideration will be restricted to symmetric potentials $\mathcal{U}(x) = \mathcal{U}(-x)$. Since BO exist in

the linear regime it is appropriate to start our considerations from the underlying linear eigenvalue problem $-d^2\varphi_q/dx^2 + \mathcal{U}(x)\varphi_q = \varepsilon(q)\varphi_q$, where φ_q is the standard Bloch function corresponding to the wave vector q . The periodicity of the linear OL introduces a band structure in the spectrum e.g. the existence of chemical potential functions $\varepsilon_n(q)$ which are periodic in reciprocal space $q \in [-1, 1]$, with n denoting the band index. In the following we shall consider only the lowest chemical potential band, a situation typical for most BEC applications, and omit the band index. In presence of nonlinearity, stationary localized states (gap-solitons) can exist only if chemical potentials are inside gaps (see e.g. [18]). This is not the case of a nonstationary (moving) soliton whose velocity, in the leading order, coincides with the group velocity of the carrier Bloch wave and mathematically can be described by a multiple-scale expansion provided the linear force is weak enough $\gamma^{1/2} \ll 1$. To this regard we search for localized solutions of Eq.(1) in the form $\psi = \gamma^{1/2}\psi_1 + \gamma\psi_2 + \dots$, where at each order ψ_j denotes a function of a set of scaled temporal $t_n = \gamma^{n/2}t$ and spatial $x_n = \gamma^{n/2}x$ ($n = 1, 2, \dots$), variables. Since for BO the solution, thought as a wavepacket of Bloch states φ_q with the carrier wave-vector depending on the slow time $q = q(\gamma t)$, must scan the whole band, the ansatz for the first order ψ_1 is chosen, in analogy with the Houston functions [19] of the underlying linear theory, of the form

$$\psi_1 = A(\tau, \xi)e^{i\mathcal{E}(t)}\varphi_{q(\tau)}(x) \quad (2)$$

where the phase $\mathcal{E}(t)$ is determined by the equation $d\mathcal{E}/dt = \varepsilon(q(\gamma t))$ and we have introduced specific notations for the slow variables $\tau = \gamma t$ and $\xi = \sqrt{\gamma}(x - v(\tau)t)$. This peculiarity of the asymptotic expansion will manifest at the third order of the small parameter, i.e. $\mathcal{O}(\gamma^{3/2})$, lower orders of the expansion being obtained in standard manner (see e.g. [13]). Since the temporal dependence of the wavevector is not specified, we impose the constraint that q must follow the well known semiclassical equation for the linear BO which in our scaled variables acquires the simplest form $q = \tau$ [21]. Then, in the order $\gamma^{3/2}$ we arrive at the NLS equation for the slowly varying amplitude

$$iA_\tau + \frac{1}{2M(q)}A_{\xi\xi} - \chi(q)|A|^2A = 0. \quad (3)$$

Here we defined the group velocity $v(q) = d\varepsilon(q)/dq$, the effective mass $M(q) = (2d^2\varepsilon(q)/dq^2)^{-1}$ and the effective nonlinearity $\chi(q) = \int_0^\pi \mathcal{G}(x)|\varphi_{q(\tau)}(x)|^4 dx$. We emphasize that although we have indicated q as an argument in the above definitions, the group velocity, the effective mass and the effective nonlinearity are functions of the slow time τ . Introducing "+" and "-" subindexes to denote properties at top and bottom limits of the band, we have that $\varphi^{(-)} = \varphi_{q=0}$, $\varphi^{(+)} = \varphi_{q=1}$, $\chi^{(\pm)} = \int_0^\pi \mathcal{G}(x)|\varphi^{(\pm)}(x)|^4 dx$, and $\mp M^{(\pm)} > 0$. As it is

clear, if $\mathcal{G}(x) = \text{const}$, then $\chi^{(+)}\chi^{(-)} > 0$ and from Eq.(3) it follows that while envelope solitons are available at one edge of the band (the edge for which $M\chi < 0$), they cannot exist at the other edge. Since for BO the soliton must travel along the whole band, it will necessarily reach the edge where it undergoes strong dispersion (due to defocusing action of nonlinearity ($M\chi > 0$), this leading to destruction of BO [15]).

From this analysis it is clear that an essential control parameter of the problem is $\sigma(q) = -M(q)\chi(q)$ and in order to have long-living BO we must require that $\sigma(q) > 0$ for all q , this assuring a focusing nonlinearity for the soliton dynamics along the whole band. The above condition can be achieved by means of a proper design of the nonlinear lattice and will be optimized if the condition $\sigma = \text{const} > 0$ is satisfied. Analytically it is easy to consider the general case in which $\sigma(\tau)$ is a slowly varying function $|d\sigma/dq| \ll \sigma$. Indeed, introducing the new temporal variable $\tilde{\tau} = \int_0^\tau d\tau'/M(\tau')$ and the new function $\mathcal{A} = A/\sqrt{\sigma}$ we obtain the NLS equation with a dissipative term $iA_{\tilde{\tau}} + \frac{1}{2}\mathcal{A}_{\xi\xi} + |\mathcal{A}|^2\mathcal{A} = i\frac{2}{\sigma}\frac{d\sigma}{dq}\mathcal{A}$ whose approximate solution can be found by means of soliton perturbation theory [20]. For the particular case of a static soliton in the frame moving with the velocity $v(\tau)$, the solution reads $\mathcal{A} = \mathcal{A}_0 \exp\left(\Gamma(\tilde{\tau}) + \frac{i}{2}\mathcal{A}_0^2 \int_0^{\tilde{\tau}} \sqrt{\sigma(\tau')}d\tau'\right) \text{sech}(\mathcal{A}_0[\sigma(\tilde{\tau})]^{1/4}\xi)$ with \mathcal{A}_0 the constant amplitude of the soliton.

In order to check the above predictions we have performed direct numerical simulations of Eq. (1) with $\mathcal{U}(x) = -V \cos(2x)$ and $\mathcal{G}(x) = G_0 + G_1 \cos(2x)$, where V and G_1 denote the amplitudes of the linear and nonlinear lattices, respectively, G_0 is the "average" nonlinearity, which in all numerical simulations reported below is chosen to be $G_0 = -0.777$. We denote by $G_1^{(\pm)}$ the value of G_1 at which effective nonlinearity $\chi^{(\pm)}$ becomes zero. Respectively if $G_1 \geq G_1^{(\pm)}$ we have that $\chi^{(\pm)} \geq 0$ and the condition for the existence of envelope solitons (alternatively, the instability of the Bloch waves) at the both band edges $M^{(\pm)}\chi^{(\pm)} < 0$ is met when $G_1^{(+)} < G_1 < G_1^{(-)}$. This corresponds to the domain of parameters between the lines in Fig.1 where $G_1^{(\pm)}$ vs V are depicted (e.g. point B in Fig.1). Consequently, domains of parameters $G_1 < G_1^{(+)}$ (e.g. point A in Fig.1) and $G_1 > G_1^{(-)}$ (e.g. point C in Fig.1) allow for the existence of small amplitude envelope solitons only at lower or upper band edge, correspondingly. Thus long-lived BOs can be expected in the domain of parameters between the two curves $G_1^{(\pm)}(V)$ in Fig.1.

Below we concentrate on the choice of the parameters corresponding to the specific points A, B, and C, in Fig. 1a. These are situations deviating from the optimally designed lattices, as is clearly seen in panels (b) and (c) of Fig.1. Indeed, while the points q_M and q_X are relatively close to each other, they do not exactly coincide,

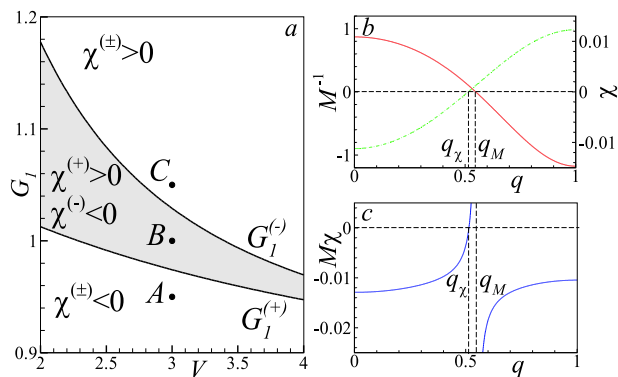


FIG. 1: (a) $G_1^{(\pm)}$ vs V which separate domains where $\chi^{(\pm)}(V) \geq 0$. The points A, B, and C correspond to the parameters explored below in Fig.2b (point A), Fig.2a and 3a (point B), and Fig.3b (point C). Long living BO can be observed in the shadowed domain. (b) The inverse effective mass M^{-1} (solid line) and the effective nonlinearity χ (dashed-dotted line) vs q . (c) $M\chi$ vs q for the parameters corresponding to the point B (panel a). $q_\chi \approx 0.5145$ and $q_M \approx 0.5475$ indicate the values of q , where χ and M^{-1} are respectively equal to zero.

what results in the singularity of $\sigma(q)$ at the point q_M and in the existence of the interval $q_\chi < q < q_M$ where envelope solitons do not exist (however outside this interval σ is a relatively slow function of the wavevector).

In Fig.2a we present the time evolution of a small amplitude envelope soliton obtained by direct numerical integration of Eq.(1). As initial condition we used the stationary envelope soliton of Eq. (1) with $\gamma = 0$, whose chemical potential belongs to the semi-infinite gap very close to the lowest allowed band. From this figure the existence of long-living BO with the period $T_s \approx 2 \cdot 10^3$ and spatial amplitude $X_s \approx 32.5\pi$, perfectly matching the semiclassical estimates $2/|\gamma|$ and $(\varepsilon^{(+)} - \varepsilon^{(-)})/(2|\gamma|)$, respectively, is quite evident. Notice that the turning points of the spatial dynamics correspond to values of chemical potentials inside the gaps (very close to band edges) for which stationary solitons exist. In Fig.2c we have compared the shape of the soliton at the fifth right turning points of the BO with the profile of the stationary state at the top of the band, from which we see that they practically coincide (the small difference is ascribed to the radiative effects of the BO dynamics). Remarkably accurate prediction of the theory is verified by comparing the dynamical profiles of the soliton at the turning points of the BO. The profiles at the times $t = 10^3$; $3 \cdot 10^3$; $5 \cdot 10^3$; $7 \cdot 10^3$ were practically indistinguishable from the one depicted for $t = 9 \cdot 10^3$ in Fig.2c. Numerical simulations performed on longer time scales (up to $t = 2 \cdot 10^4$) showed no appreciable decay of the BO and perfect recovering of the soliton shape at the turning points.

To appreciate the importance of the parameter design

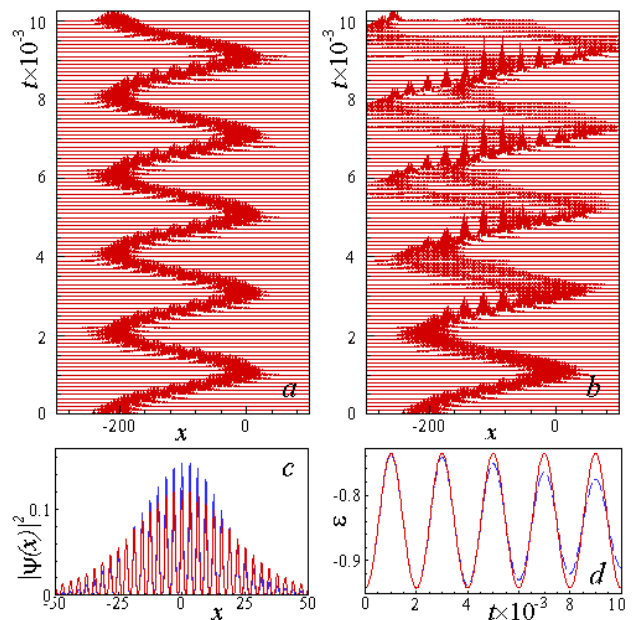


FIG. 2: (Color online) (a) Long-living BO of the envelope soliton for $G_1 = 1.0$ (corresponding to point B in Fig.1a). (b) Decaying BO for $G_1 = 0.95$ (corresponding to point A in Fig.1a). In both cases oscillations start near the bottom of the band at $\varepsilon = -0.938$ with parameter values $\gamma = -0.001$, $V = 3.0$ and with initial condition $X_0 = -65\pi$. (c) The shape of the envelope soliton in panel (a) at time $t = 9000$ (thin solid lines) is compared with the stationary state (thick solid lines) with the same number of particles $N = 2.42$ and chemical potential nearby the upper edge of the band at $\varepsilon = -0.7324$. (d) The chemical potential $\varepsilon(t)$ for long-living ($G_1 = 1.0$, solid line) and decaying ($G_1 = 0.95$, dashed line) BO. The lowest allowed band corresponds to the interval $\varepsilon \in [-0.93683, -0.73326]$.

implied by our theory, we depict in Fig.2b the dynamics of a soliton corresponding to point A in Fig.1. We see that in this case the BO undergo fast decay due to spreading of the wave packet. The difference in the two types of BO is clearly seen also from the dependence of the chemical potential on time, computed as $\varepsilon(t) = \frac{1}{N} \int_{-\infty}^{\infty} (|\psi_x|^2 + \mathcal{U}(x)|\psi|^2 + \mathcal{G}(x)|\psi|^4) dx$, with $N = \int_{-\infty}^{\infty} |\psi|^2 dx$ denoting the number of atoms. This is shown in Fig.2d from which we see that stable BO correspond to perfectly periodic trajectory (solid line) while decaying oscillations correspond to decays of the oscillations of the chemical potential (dashed line). Similar phenomena exist also if the BO is started from stationary states at the top, rather than at the bottom, of the band for the same parameter values of points B, C, in Fig.1a), as one can see from Fig.3.

In closing this letter we wish to discuss possible experimental settings for observing long-living BO in BECs trapped in uniformly accelerated linear and nonlinear OLs (with acceleration 2γ): $\mathcal{U}(X - \gamma T^2)$ and $\mathcal{G}(X - \gamma T^2)$, respectively. The corresponding model equation in di-

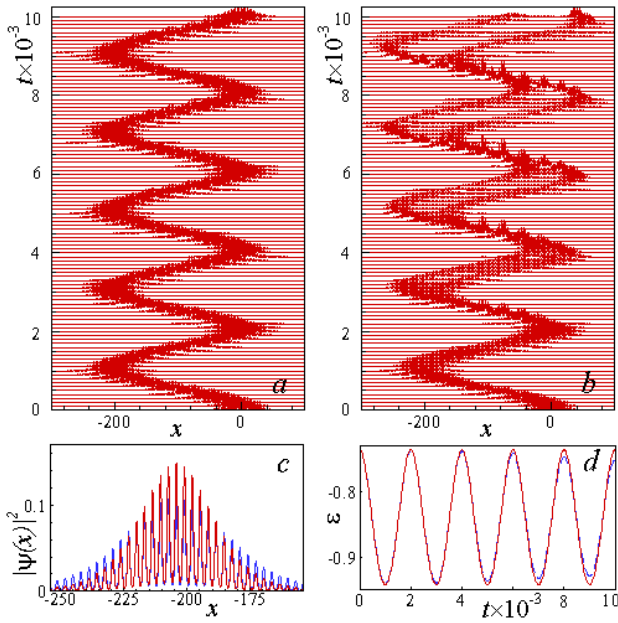


FIG. 3: (Color online) Dynamics of BO for the cases (a) $G_1 = 1.0$ and (b) $G_1 = 1.05$ (corresponding, respectively, to points B and A in Fig.1a). In both cases the oscillations start near the top of the band at $\varepsilon = -0.7324$, with $\gamma = -0.001$, $V = 3.0$ and initial condition $X_0 = 0\pi$. In (c) we compare the profile of the soliton at $t = 9 \cdot 10^3$ in panel (a) (thin solid lines) with the stationary solution (thick solid lines) with the same number of particles $N = 2.42$ and belonging to the semi-infinite gap ($\varepsilon = -0.938$). In (d) the dynamics of the chemical potential $\varepsilon(t)$ is shown for $G_1 = 1.0$ (solid line) and $G_1 = 1.05$ (dashed line).

dimensionless variables takes the form

$$i\Psi_T = -\Psi_{XX} + \mathcal{U}(X - \gamma T^2)\Psi + \mathcal{G}(X - \gamma T^2)|\Psi|^2\Psi. \quad (4)$$

After substituting $\psi = e^{-i[(X - \gamma T^2)\gamma T + \gamma^2 T^3/3]}\Psi$ and introducing new independent variables $x = X - \gamma T^2$ and $t = T$, Eq. (4) takes the form of a NLS equation with external linear force (1). In this normalization the energy is measured in units of the recoil energy $E_r = \hbar^2 \pi^2 / (2md^2)$, where d is the lattice period and m is the mass of bosons, and the spatial and temporal variables are measured in units of d/π and \hbar/E_r , respectively. To check the experimental feasibility of the proposed setting, we consider a ^{87}Rb condensate in a trap with a transverse radial size $a = 2 \mu\text{m}$ and with a period of linear and nonlinear lattices $d = 1 \mu\text{m}$. Then dimensionless parameters of long-living BO, depicted in Fig.2a and 3a will correspond to soliton, containing $N \approx 3800$ atoms, driven by external force $1.17 \cdot 10^{-27}\text{N}$ (which is obtained, when the acceleration of linear and nonlinear lattices is of order of $\sim 8\text{mm/s}$). At the same time the above parameters of the nonlinear lattice could be created by the spatial variation (obtained by the optically induced Feshbach resonance) of the bosonic s-wave scattering length $a_s(x) = a_s^{(0)} + a_s^{(1)} \cos(2\pi x/d)$ with the "average" value

$a_s^{(0)} = -1.554\text{nm}$ and the amplitude $a_s^{(1)} = 2\text{nm}$. For the parameters of Fig.1, the long-living BO will occur when the amplitude of the spatial variation of the scattering length is in the range $1.948\text{nm} < a_s^{(1)} < 2.058\text{nm}$. This shows that the long lived BO reported in this Letter can indeed be observed in the experimental settings available today.

M.S. acknowledges support from a MUR-PRIN-2005 initiative *Transport properties of classical and quantum systems*. VVK was supported by the FCT and European program FEDER under Grant No. POCI/FIS/56237/2004. Y.V.B. acknowledges support of the FCT under the Grant No. SFRH/PD/20292/2004.

-
- [1] Bloch F. Z. Phys. **52** (1928) 555
 - [2] see e.g the review by Karl Leo, Semicond. Sci. Technol. **13** (1998) 249263 and references therein.
 - [3] U.Peschel, T.Persch, and F.Lederer, Opt. Lett. **23**, 1701 (1998).
 - [4] H. Trompeter, *et al.*, Phys. Rev. Lett. **96**, 053903 (2006)
 - [5] D.-I. Choi and Q. Niu, Phys. Rev. Lett. **82**, 2022 (1999)
 - [6] O. Morsch, *et al.*, Phys. Rev. Lett. **87**, 140402 (2001); M. Cristiani, *et al.*, Phys. Rev. A **65**, 063612 (2002)
 - [7] A. R. Kolovsky and H. J. Korsch, Int. J. Mod. Phys. B **18**, 1235 (2004).
 - [8] R. Battesti, *et al.*, Phys. Rev. Lett. **92**, 253001 (2004); P. Clad, *et al.*, Phys. Rev. A **74**, 052109 (2006).
 - [9] I. Carusotto, *et al.*, Phys. Rev. Lett. **95**, 093202 (2005).
 - [10] G. Ferrari, N. Poli, F. Sorrentino, and G. M. Tino, Phys. Rev. Lett. **97**, 060402 (2006).
 - [11] S. Longhi, Phys. Rev. E **75**, 026606 (2007).
 - [12] M. Bruschi, D. Levi, and O. Ragnisco, Nuovo Cimento, **53A**, 21 (1979); R. Sharf and A. R. Bishop, Phys. Rev. A **43**, 6535 (1991); V. V. Konotop, O. A. Chubykalo, and L. Vázquez, Phys. Rev. E **48**, 563 (1993); D. Cai, *et al.*, Phys. Rev. Lett. **74**, 1186 (1995).
 - [13] V.V. Konotop and M. Salerno, *Phys. Rev.* **A65**, 021602 (2002).
 - [14] B. Wu and Q. Niu, Phys. Rev. A **64**, 061603 (2001); B. B. Baizakov, V. V. Konotop, and M. Salerno, J. Phys. B, **35**, 5105 (2002); M. Machholm, C. J. Pethick, and H. Smith, Phys. Rev. A **67**, 053613 (2003). L. De Sarlo, *et al.*, Phys. Rev. A **72**, 013603 (2005).
 - [15] L. Fallani, *et al.*, Phys. Rev. Lett. **93**, 140406 (2004).
 - [16] R. G. Scott, *et al.*, Phys. Rev. Lett. **90**, 110404 (2003); R. G. Scott, *et al.*, Phys. Rev. A. **69**, 033605 (2003).
 - [17] Yu. V. Bludov, V.A. Brazhnyi, and V.V. Konotop, Phys. Rev. A **76**, 023603 (2007).
 - [18] G. L. Alfimov, V. V. Konotop, and M. Salerno, Europhys. Lett. **58**, 7 (2002).
 - [19] W. V. Houston, Phys. Rev. **57**, 184 (1940).
 - [20] V. I. Karpman and E. M. Maslov, Zh. Eksp. Teor. Fiz. **73**, 537 (1977) [Sov. Phys. JETP **46**, 281, (1977)].
 - [21] This condition allows one to cancel the third order terms originated by the temporal dependence of the wave vector $q(\gamma t)$, and is obtained formally by using that $\int_0^\pi \bar{\varphi}_q \frac{\partial}{\partial q} \varphi_q dx = \int_0^\pi x |\varphi_q|^2 dx$ for symmetric potentials.